Steric Size in Conformational Analysis. Steric Compression Analyzed by Circular Dichroism Spectroscopy

Stefan E. Boiadjiev and David A. Lightner*

Contribution from the Department of Chemistry, University of Nevada, Reno, Nevada 89557-0020

Received June 9, 2000

Abstract: The relative steric size of methyl, ethyl, isopropyl, *tert*-butyl, phenyl, and benzyl groups has been determined from a sensitive tetrapyrrole model and exciton coupling circular dichroism (CD) measurements. Unlike the classical cyclohexane model, from which the relative steric demand of functional groups has been assessed quantitatively (*A*-values) and is based on the preference for equatorial vs axial orientations, the bilirubin model assesses substituent size from head-to-head steric compression. Thus, exciton CD amplitudes of a set of sensitive *anti*-chiral α(*R/S*)-substituted-*β′*(*S*)-methylmesobilirubins-XIIIα (**1**−**6**) suggests an apparent relative steric size: *tert*-butyl ∼ isopropyl > phenyl ∼ ethyl > benzyl > methyl. The order is somewhat different from that obtained by measuring equatorial vs axial configuration preferences on substituted cyclohexanes by NMR spectroscopy: *tert*-butyl ≫ phenyl > isopropyl > ethyl ∼ benzyl ∼ methyl.

Introduction

Some 45 years ago, Winstein and Holness[1] defined the "*A*-value" of a substituent group on chair cyclohexane as the thermodynamic preference for the equatorial conformation over the axial: *A*-value $= -\Delta G_{eq}^{\circ} = (RT \ln K_{eq})/1000$ for the axial ⇆ equatorial equilibrium (Figure 1). Over the years, conformational *A*-values have been determined and compiled[2,3] for a diverse array of groups. Such tabulations of *A*-values constitute an invaluable resource for quickly (and quantitatively) assessing the relative steric size of functional groups such as alkyl, hydroxyl, halogen, etc. For example, according to their *A*-values the steric demand of a methyl group ($A_{CH_3} \sim 1.74$) is significantly greater than that of a methoxyl ($A_{OCH_3} \sim 0.75$), which is smaller than that of a methylthio ($A_{SCH_3} \sim 1.00$).[2,3]

Most substituents prefer the equatorial conformation over the axial.[2,3] This may be attributed to the nonbonded steric repulsions between an axial group and the two gauche ring methylene groups at C(3) and C(5) of chair cyclohexane. Such steric repulsions are absent for equatorial groups (Figure 1). The cyclohexane model thus assesses steric size of functional groups on the basis of gauche interactions, and as in every steric model, it assumes a fixed template, i.e., chair conformations with no ring conformational distortion introduced by the functional groups−particularly the axial substituent.

Conformational *A*-values have become the most readily available resource for predicting the relative steric demand of a variety of substituents even outside the cyclohexane framework, e.g., in situations such as molecular recognition studies, where steric demand is based more on a linear than a transverse or lateral buttressing.[4] To assess substituent steric demand in the linear or face-to-face orientation, we used circular dichroism (CD) spectroscopy to extract the steric demand of functional groups located on a very different stereochemical template from that provided by cyclohexanes, viz. the tetrapyrrole mesobilirubin-XIIIα (Figure 2). This tetrapyrrole, a synthetic analogue of bilirubin (the yellow pigment of jaundice[5]), offers a more sterically demanding molecular framework for assessing functional group steric size. Bilirubins are bichromophoric pigments, and the conformational equilibrium of interest involves interconverting conformational enantiomers where the two dipyrrinones pivot about a C(10) methylene connector (Figure 2).[6]

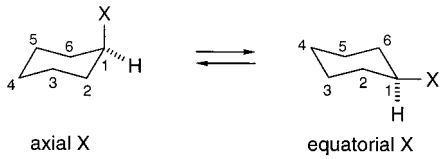

Figure 1. Cyclohexane chair−chair conformational equilibrium that interconverts axial and equatorial X groups. Gauche interactions between axial X and the C(3) and C(5) methylene group of the cyclohexane ring destabilize the axial conformer relative to the equatorial. The *A*-value for group X is defined in terms of the free energy for the equilibrium $A = -\Delta G^{\circ}_{eq} = (RT \ln K_{eq})/1000$.

Previous studies have shown that the most stable conformation of bilirubin and mesobilirubin is shaped like a ridge-tile, with the two dipyrrinones oriented nearly orthogonal. This conformation is further greatly stabilized by six intramolecular hydrogen bonds shared between each dipyrrinone and an opposing propionic acid carboxyl group (Figure 3).[6] Two enantiomeric intramolecularly hydrogen-bonded, ridge-tile conformations are possible, and they were found to interconvert at

(1) Winstein, S.; Holness, N. J. *J. Am. Chem. Soc.* **1955**, *77*, 5562−5578.

(2) Bushweller, C. H. Stereodynamics of Cyclohexane and Substituted Cyclohexanes. Substituent *A* Values. In *Conformational Behavior of Six-Membered Rings Analysis, Dynamics and Stereoelectronic Effects*; Juaristi, E., Ed.; VCH-Wiley Publ.: New York, 1995; Chapter 2.

(3) Eliel, E.; Wilen, S. H. *Stereochemistry of Carbon Compounds*; J. Wiley and Sons: New York, 1994.

(4) Rebek, J., Jr. *Acc. Chem. Res.* **1999**, *32*, 278−286. (b) Tucci, F. C.; Renslo, A. R.; Rudkevich, D. M.; Rebek, J., Jr. *Angew. Chem., Int. Ed. Engl.* **2000**, *39*, 1076−1079.

(5) McDonagh, A. F. Bile Pigments: Bilatrienes and 5,15-Biladienes. In *The Porphyrins*; Dolphin, D., Ed.; Academic Press: New York, 1979; Vol. VIA, Chapter 6, pp 293−491. (b) Chowdhury, J. R.; Wolkoff, A. S.; Chowdhury, N. R.; Arias, I. M. In *The Metabolic and Molecular Bases of Inherited Disease*; Scriver, C. R., Beaudet, A. L., Sly, W. S., Valle, D., Eds.; McGraw-Hill Inc.: New York, 1995; Vol. II, pp 2161−2208.

(6) Person, R. V.; Peterson, B. R.; Lightner, D. A. *J. Am. Chem. Soc.* **1994**, *116*, 42−59.

10.1021/ja002069c CCC: $19.00
Published on Web 11/03/2000

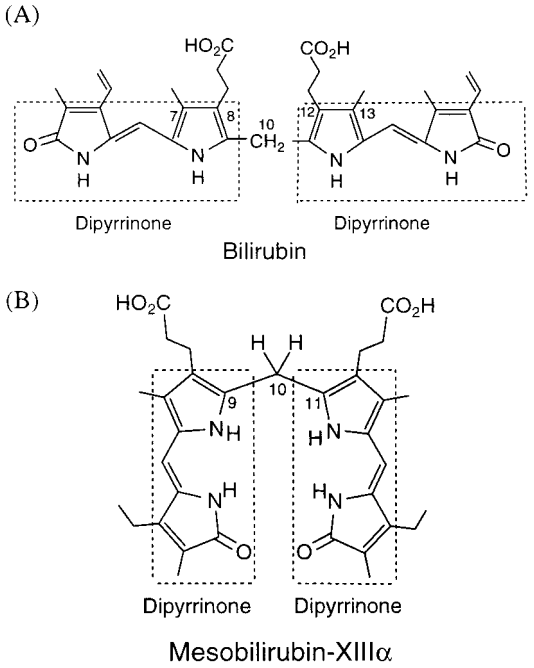

Figure 2. (A) Bilirubin in a linear conformation. (B) Mesobilirubin-XIIIα in a porphyrin-like conformation.

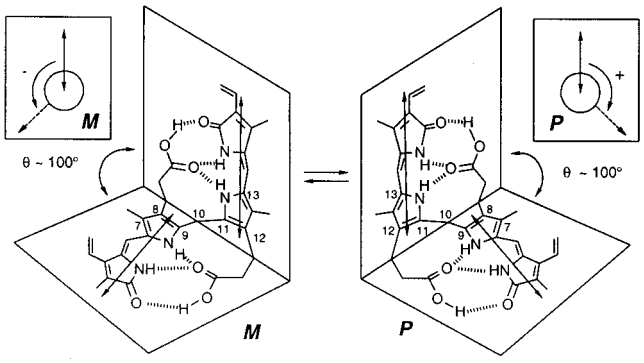

Figure 3. Interconverting intramolecularly hydrogen-bonded enantiomeric conformers of bilirubin-IXα. The double-headed arrows represent the dipyrrinone long wavelength electric transition moments (dipoles). The relative helicities (***M***, minus, or ***P***, plus) of the vectors are shown (inset) for each enantiomer. Hydrogen bonds are shown by hatched lines.

rates of 7.2 ± 0.4 s^{-1} (~53 °C)[7a] and 3−95 s^{-1} (50−95 °C)[7b] over a barrier of ~18−20 kcal/mol in a nonpolar solvent such as chloroform. Such conformational enantiomerism[8] can be tilted toward a specific enantiomer by introduction of a single methyl group on each propionic acid[9] (or even on only one propionic acid).[10] Thus, $\beta(S),\beta'(S)$- and $\alpha(S),\alpha'(S)$-dimethylmesobilirubin-XIIIα have each been shown to reside nearly exclusively in the ***M***-helical ridge-tile conformation, whereas the $\beta(R),\beta'(R)$- and $\alpha(R),\alpha'(R)$-dimethylrubins reside in the ***P***.[9a,b] This forced selection of either the ***M*** or ***P*** conformational enantiomer, for which large exciton coupling CD Cotton effects[11] have been measured, has its origins in specific intramolecular buttressing effects involving the α and β methyl groups and specific ring methyls or methylenes.[9]

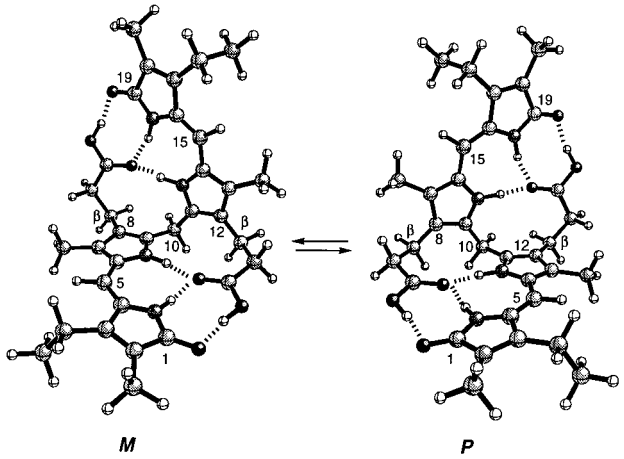

Figure 4. Ball and stick conformational representations for the ridge-tile shape ***M***- and ***P***-chirality, intramolecularly hydrogen-bonded, interconverting enantiomers of mesobilirubin-XIIIα. In the propionic acid side chains attached to pyrrole ring carbons C(8) and C(12), the hydrogens on the β and β′ $-CH_2-$ and the α,α′ $-CH_2-$ groups are either *pro-R* or *pro-S*. When the ***M***-chirality conformer inverts into the ***P***-chirality, steric crowding of the *pro-R* hydrogens is relieved and replaced by similar crowding of the *pro-S* hydrogens.

In the ***M*** conformer of mesobilirubin-XIIIα, the *pro-R* hydrogens of the propionic acid α and β carbons exsert into the ring methyls at C(7)/C(13) and the C(10) methylene, respectively, but the *pro-S* hydrogens are free of nonbonded steric compression (Figure 4).[6,9] In contrast, in the *P* conformer, the *pro-S* hydrogens lie in the more sterically congested environment, while the *pro-R* are unstrained. Consequently, when a substituent larger than hydrogen is present on the α or β stereogenic center of the propionic acid group, the ***M*⇆*P*** conformational equilibrium is directed toward either the ***M*** helical conformer or the ***P***, depending on the stereochemistry at α or β. With an $\alpha(S)$ or $\beta(S)$ methyl substituent, for example, the favored conformer is ***M***, and with $\alpha(R)$ or $\beta(R)$, the favored conformer is ***P***.[6,9] Thus, $(\beta S,\beta' S)$-dimethylmesobilirubin-XIIIα is computed to be some 4−5 kcal/mol more stable in the ***M*** helical conformation than in the ***P***,[6,9a] because in the latter the β-methyls are sterically compressed into the C(10) methylene group. This chirognostic interplay between nonbonded steric interaction and pigment conformation is possible only in the intramolecularly hydrogen-bonded ridge-tile conformation, and it has been used recently to compare the relative effectiveness of steric buttressing from α and β methyls [9d] and to evaluate the relative size of OCH_3 and SCH_3 groups.[12]

In the following, we report on a novel determination of the relative steric size of methyl, ethyl, isopropyl, *tert*-butyl, phenyl, and benzyl groups from CD spectroscopy of new synthetic bilirubins **2**−**6**, each with an α-substituent in one propionic acid chain and a $\beta'(S)$ methyl group in the other propionic group. The templates are the interconverting, intramolecularly hydrogen-

(7) Manitto, P.; Monti, D. *J. Chem. Soc. Chem. Commun.* **1976**, 122−123. (b) Navon, G.; Frank, S.; Kaplan, D. *J. Chem. Soc., Perkin Trans. 2* **1984**, 1145−1149.

(8) Lightner, D. A.; Gawronski, J. K.; Gawronska, K. *J. Am. Chem. Soc.* **1985**, *107*, 2456−2461. (b) Reisinger, M.; Lightner, D. A. *J. Inclusion Phenom.* **1985**, *3*, 479−486. (c) Lightner, D. A.; Gawronski, J. K.; Wijekoon, W. M. D. *J. Am. Chem. Soc.* **1987**, *109*, 6354−6362.

(9) Boiadjiev, S. E.; Person, R. V.; Puzicha, G.; Knobler, C.; Maverick, E.; Trueblood, K. N.; Lightner, D. A. *J. Am. Chem. Soc.* **1992**, *114*, 10123−10133. (b) Puzicha, G.; Pu, Y.-M.; Lightner, D. A. *J. Am. Chem. Soc.* **1991**, *113*, 3583−3592. (c) Boiadjiev, S. E.; Lightner, D. A. *Tetrahedron: Asymmetry* **1996**, *7*, 1309−1322. (d) Boiadjiev, S. E.; Lightner, D. A. *Tetrahedron: Asymmetry* **1997**, *8*, 2115−2129. (e) Bauman, D.; Killet, C.; Boiadjiev, S. E.; Lightner, D. A.; Schönhofer, A.; Kuball, H.-G. *J. Phys. Chem.* **1996**, *100*, 11546−11558.

(10) Boiadjiev, S. E.; Lightner, D. A. *Tetrahedron: Asymmetry* **1997**, *8*, 3603−3615.

(11) Harada, N.; Nakanishi, K. *Circular Dichroism Spectroscopy-Exciton Coupling in Organic Stereochemistry*; University Science Books: Mill Valley, CA, 1983.

(12) Boiadjiev, S. E.; Lightner, D. A. *Chirality* **2000**, *12*, 204−215.

bonded ridge-tile conformational enantiomers of Figure 3, and the intrinsic, nonbonded face-to-face steric compression.

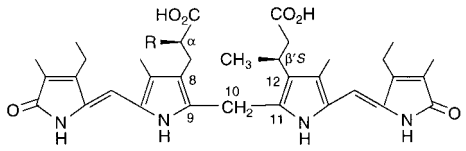

1: R = CH_3 **2**: R = CH_2CH_3

3: R = $CH(CH_3)_2$ **4**: R = $C(CH_3)_3$

5: R = C_6H_5 **6**: R = $CH_2C_6H_5$

Synthesis. Our synthetic strategy[13] for preparing rubins **1**−**6** followed the design and methodology used previously in the syntheses of optically active, nonsymmetrically substituted mesobilirubins.[9d,10] The general plan involved chloranil-promoted oxidative coupling (Scheme 1) of two different dipyrrinones, one with a β-methyl substituent in the propionic acid group (**36** or **37**), the other with an α-substituent (**27**−**35**), to give tetrapyrrole verdin precursors of **1**−**6**. Although the coupling is expected to give a 1:2:1 statistical mixture of α,α′:α,β′:β,β′ disubstituted verdins, from which the desired α,β′ isomer must be isolated, sufficiently differing polarities were engineered into the three verdins so as to facilitate chromatographic separation. This was achieved simply by coupling dipyrrinone acids and esters, which always affords the target α,β′ disubstituted verdin (**13**−**18**) as a monoester, and is accompanied by an (α,α′ + β,β′) disubstituted verdin diacid (**25** or **21**−**23**) and verdin diester (**26** or **19**, **20**, **24**). Typically the verdin monoester had a polarity intermediate between the diacid and diester and was isolated by radial chromatography on silica gel by eluting with CH_2Cl_2–CH_3OH (gradient 98.5:1.5 to 95:5 by volume) to give isolated yields of pure **13**−**18** varying from 66 to 80% of the statistical theoretical yield.

To have optically active final products and avoid multiple optical resolutions at the final product stage, it was important that one of the coupling partners be an optically active dipyrrinone. For what would become the right half of verdins **13**−**18**, we chose β(*S*)-xanthobilirubic acid (**36**) or its methyl ester (**37**), as both were available in 100% ee and known absolute configuration from earlier studies.[9a,10] Thus, **36** or **37** served as the vehicle for ensuring high ee and known absolute configuration in the desired verdin. For the left half of the target verdins we required dipyrrinone coupling partners (**27**−**35**) that were, except for **27**,[9b] unknown when we commenced this study. Some presented special synthetic challenges, particularly those with bulky *tert*-butyl (**31**, **32**) and phenyl (**33**, **34**) groups. All were racemic mixtures, thus ensuring that the desired verdin products **13**−**18** would be diastereomeric mixtures. We assumed that a 50:50 mixture of verdin diastereomers would be formed and found that in most cases it varied from 45:55 to 55:45, as determined by NMR spectroscopy.

Separation of the diastereomers was not achieved at the verdin stage but was accomplished after conversion to rubins (Scheme 2). Thus verdin monoesters **13**−**18** were saponified to diacids, which were reduced to rubins using $NaBH_4$. The saponification step dictated a choice of dipyrrinone acid (**29**, **31**, **33**) rather than ester (**30**, **32**, **34**) for the left-half coupling partner, since propionate esters with α-isopropyl, *tert*-butyl, or phenyl groups resisted hydrolysis (as expected). Saponification of **30** to **29** or **34** to **33**, for example, required forcing conditions (aqueous ethanolic NaOH at reflux for 9 h), treatment unsuitable for saponifying sensitive verdin esters. However, **32** resisted saponification, even under these forcing conditions, but it was converted to acid **31** by heating at reflux in *s*-collidine with anhydrous LiI.[14] In reactions where dipyrrinone acids **29**, **31**, and **33** were used to make verdin monoesters **15**−**17**, the right-half coupling partner became dipyrrinone ester **37**. The verdin diacids obtained by simple saponification of monoesters **13**−**18** were then smoothly reduced to the corresponding rubin diastereomers by $NaBH_4$ in methanol, as seen by the initially

Scheme 1

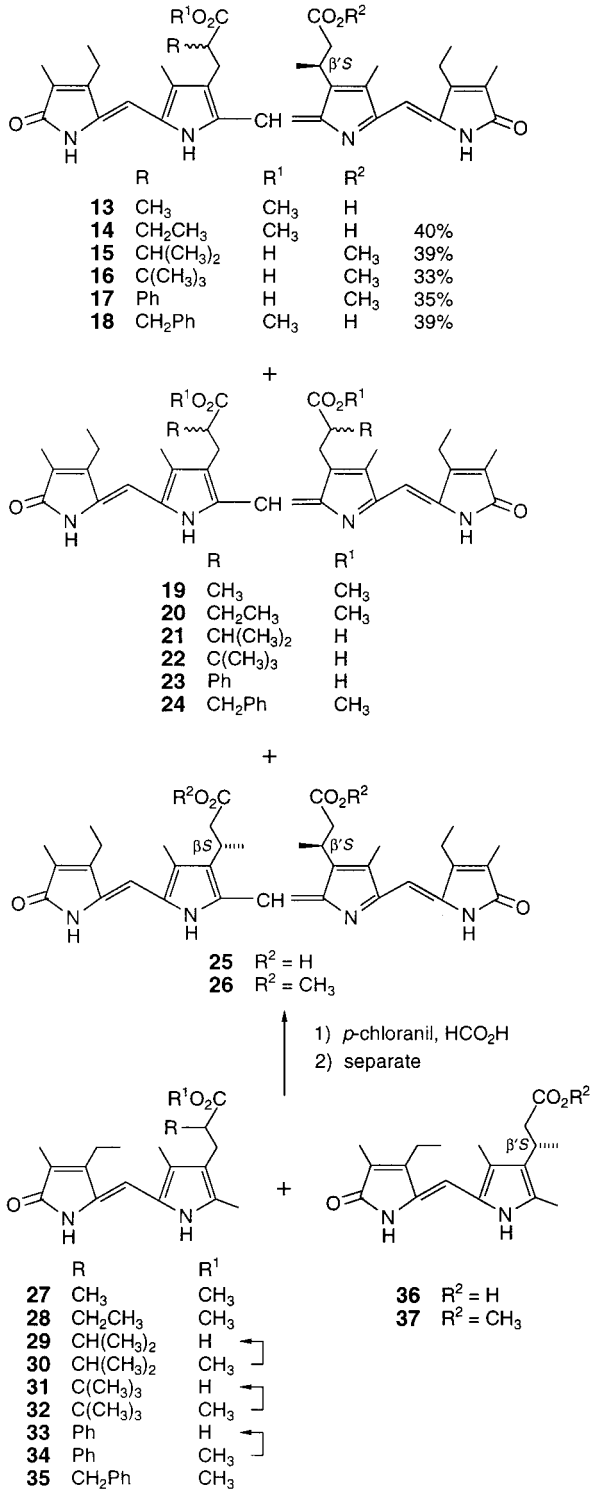

(13) Boiadjiev, S. E.; Lightner, D. A. *Synlett* **1994**, 777−785.

(14) Elsinger, F.; Schreiber, J.; Eschenmoser, A. *Helv. Chim. Acta* **1960**, *43*, 113−118.

Scheme 2

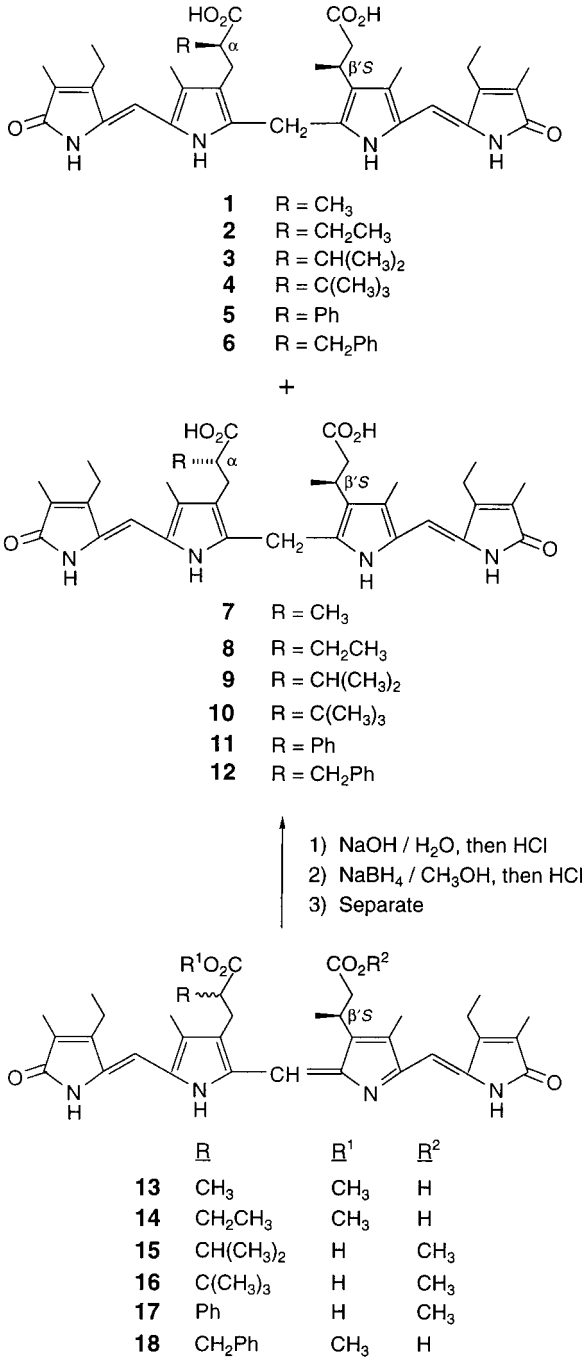

blue-green verdin solutions becoming bright yellow. The resulting mixture of diastereomeric rubins was in each case separated by radial chromatography on silica gel using (0.6−1.5% by volume) CH_3OH in CH_2Cl_2. Diastereomers **1**−**6** were more polar than **7**−**12**, which provided an indication of product stereochemistry: that the α and β' stereocenters of **1**−**6** had the opposite chiral sense while those of **7**−**12** had the same.

Although the right-half dipyrrinone coupling partner (**36** or **37**) was available from earlier studies,[9a,10] the left-half dipyrrinones (**28**−**35**) were unknown. Their syntheses followed a standard dipyrrinone preparation methodology (Scheme 3):[15,16] reaction of 3-methyl-4-ethyl-5-bromomethylenepyrrolinone (**46**)[16] with a 5-H monopyrrole, generated in situ from the pyrrole α-carboxylic acids derived from monopyrroles **38**−**42**. The key steps in the preparation of the mesobilirubins **2**−**6** and **8**−**12** thus became the syntheses of monopyrroles **38**−**42**. Synthesis

Scheme 3

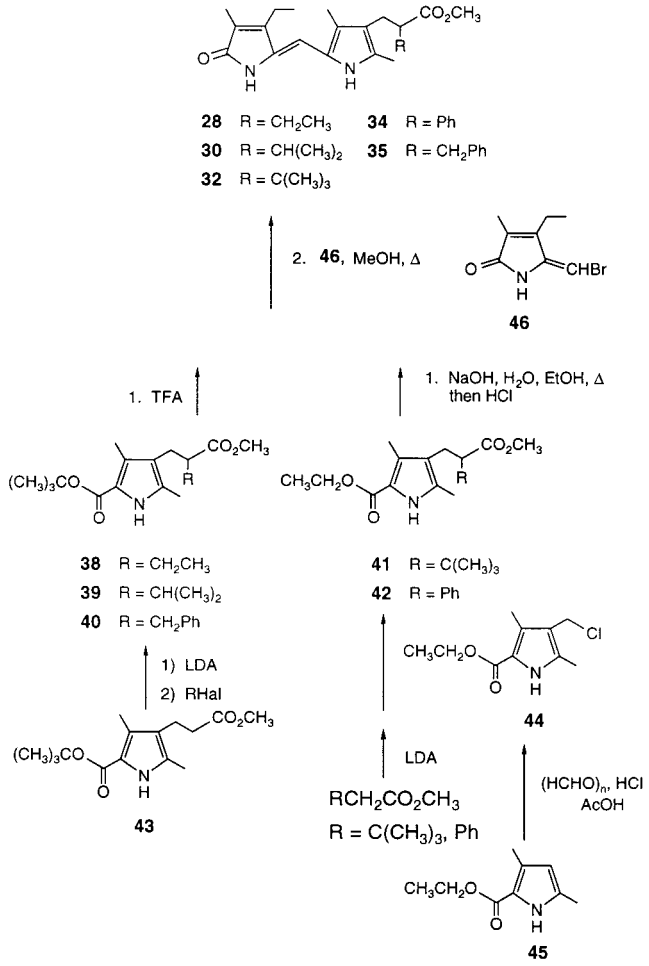

of the α-ethyl (**38**), α-isopropyl (**39**), and α-benzyl (**40**) monopyrroles was accomplished by alkylation of the propionic ester group of the known monopyrrole **43**.[17] Thus, alkylation of the ester enolate generated in THF at −60 °C from the NH-unprotected pyrrole (both α-CH_2–CO_2R and NH deprotonation) with 2.4 equiv of LDA,[12,18] followed by reaction with ethyl iodide at −78 °C, gave almost complete conversion to **38**. Crystallization of the crude product removed unreacted **43** (∼3%), affording pure **38** in 72% yield. Use of ethyl bromide in place of ethyl iodide was less satisfactory, with ∼15% unreacted starting material that is difficult to remove by crystallization of the mixture with **38**. Treatment of **38** with TFA deprotected the *tert*-butyl ester, and the resulting acid was reacted with **46** in refluxing methanol to afford dipyrrinone **28** in 63% yield.

Similarly, reaction of **43** with LDA,[18] then with benzyl bromide gave **40** in 83% isolated yield. Like **38**, the β-methylene protons of the propionate ester ABX spin system of **40** appeared (at 2.54 and 2.94 ppm) with nearly averaged coupling constants: $^3J = 5.7$ and 7.6 Hz. Again, deprotection of the *tert*-butyl ester followed by coupling with **46** afforded dipyrrinone

(15) Falk, H. *The Chemistry of Linear Oligopyrroles and Bile Pigments*; Springer-Verlag: Vienna, 1989.

(16) Shrout, D. P.; Lightner, D. A. *Synthesis* **1990**, 1062−1065. (b) Trull, F. R.; Franklin, R. W.; Lightner, D. A. *J. Heterocycl. Chem.* **1987**, *24*, 1573−1579. (c) Lightner, D. A.; Ma, J.-S.; Adams, T. C.; Franklin, R. W.; Landen, G. L. *J. Heterocycl. Chem.* **1984**, *21*, 139−144.

(17) Smith, K. M.; Pandey, R. K. *J. Heterocycl. Chem.* **1983**, *20*, 1383−1388. (b) Johnson, A. W.; Kay, I. T.; Markham, E.; Price, R.; Shaw, K. B. *J. Chem. Soc.* **1959**, 3416−3424.

(18) Boiadjiev, S. E.; Lightner, D. A. *Synlett* **1997**, 1277−1278.

35 in 67% isolated yield. And, like the monopyrroles **38** and **40**, averaged coupling constants (^3J) in the propionate chain of **35** (as well as **28**) indicated conformational mobility.

Alkylation of **43** with isopropyl iodide in THF, as above, failed to give the expected isopropyl pyrrole **39**. However, with added HMPA cosolvent, which had been shown to promote alkylations with secondary alkyl halides,[19] a 83% yield of pure **39** was achieved. Conversion of **39** to **30**, as for **28** and **35**, proceeded uneventfully in 48% yield. Unlike **38** and **40**, analysis of the $^1H\{^1H\}$ coupling constants of the propionate ester chain of **39** revealed a strong conformational preference. One of the diastereotopic β-methylene protons of **39** showed $^3J = 4.7$ Hz, indicative of gauche vicinal local stereochemistry. The other showed $^3J = 10.5$ Hz, characteristic of an antiperiplanar orientation. The same sort of conformation restriction was observed in the propionate chain of dipyrrinone **30** but not in dipyrrinones **28** and **35**.

The procedure used above to introduce the propionate α-alkyl groups in **38**−**40** could not be used to introduce the *tert*-butyl and phenyl substituents. The preparation of **41** and **42** required alternative methods. In one approach toward converting **43** to **42**, we investigated a Friedel−Crafts alkylation of methyl 2,4-dimethyl-3-(2-bromo-2-carbomethoxyethyl)pyrrolecarboxylate[18] with benzene in the presence of anhydrous $AlBr_3$. While the desired substitution of phenyl for bromine was accomplished, the $AlBr_3$ also apparently cleaved the pyrrole 2-carbomethoxy group to give the 2-carboxylic acid. The yield of desired product was too low (39%), and its purification was too tedious for our purposes; so, an alternative procedure was developed for preparing both **42** and **41**.

Rather than attempting to alkylate or arylate a pyrrole 3-propionate ester, the successful alternative pathway involved reaction of chloromethylpyrrole **44** with the ester α-anions prepared by treating either methyl neohexanoate[20] (to give **41**) or methyl phenylacetate (to give **42**) with LDA. We were pleased to find that these reactions proceeded smoothly and afforded satisfactory isolated yields (45−51%) of **41** and **42** despite severe steric hindrance at the chloromethyl group from the adjacent ring methyls − a situation akin to the *ortho* steric effect in 2,6-dimethylbenzene compounds[21] where reactions at carbon attached to C(1) are extremely difficult. (Chloromethyl)-pyrrole **44**[22] is very reactive and tricky to prepare. Its synthesis had been reported earlier only once[22] and involved reaction of the readily available 4-H pyrrole **45**[23] with paraformaldehyde in glacial acetic acid saturated with HCl gas. The reaction is capricious and must be controlled carefully, as the product (**44**) is very sensitive toward solvolysis. Failure to control the reaction properly leads to formation of bis(5-carboethoxy-2,4-dimethyl-3-pyrryl)methane as the major product, a substance first synthesized long ago by Fischer and Nenitzescu.[24]

To prepare **41** and **32**, the ester enolate of methyl neohexanoate was generated in THF at −5 °C and reacted with **44** in the presence of HMPA at −78 °C and allowed to reach ambient temperature. The conditions were optimized by using excess enolate, as any unreacted **44** present during the work up produces a dipyrrylmethane (see above) that is removed only by a tedious chromatography. The 2-carboethoxy group of **41** was saponified in a refluxing solution of NaOH in aqueous ethanol, and the product was reacted directly with **46** in refluxing methanol to give dipyrrinone **32** in 80% yield. Both monopyrrole **41** and dipyrrinone **32** exhibited restricted motion in the methyl propionate chain, as evidenced by its ^1H NMR vicinal coupling constants: $^3J = 2.9$ and 12.2 Hz in **41** and 2.8 and 12.0 Hz in **32**.

Introduction of an α-phenyl group in **42** was achieved as above for *tert*-butyl. Thus, the enolate formed by reaction of methyl phenylacetate with LDA in THF at −50 °C was reacted with β-(chloromethyl)pyrrole **44** in THF−HMPA at −78 to −40 °C to give a 51% of **42**. After saponification, **42** was condensed with **46** in refluxing methanol to afford pure dipyrrinone **34** in 58% isolated yield. The ^1H NMR spectra of both **42** and **34** gave no evidence for restricted motion in the propionic ester chain, as had been observed for the isopropyl and *tert*-butyl analogues, **39**, **41**, **30,** and **32**.

With the required left-half dipyrrinones (**28**, **30**, **32**, **34**, **35**) now available, we were ready to take them on the path to verdin monoesters **13**−**18** by oxidative coupling with dipyrrinone acid **36** (Scheme 1). However, while we anticipated (and observed) no difficulty in saponifying verdins **13**, **14,** and **18** to verdin diacids (or rubin diacids), we were concerned that the saponification or hydrolysis of the more hindered verdin monoesters (**15**, **16**, **17**) would prove resistant to or require conditions that would destroy the sensitive verdin or rubin structure. (For example, nucleophilic attack at C(10) in verdins is well documented.[15]) In such cases, it seemed wiser to accomplish the ester to acid conversion on the more robust dipyrrinones, e.g., **30** → **29**, **32** → **31** and **34** → **33** (Schemes 1 and 3) and then oxidatively couple these left half dipyrrinone acids with dipyrrinone *ester* **37**. The resulting verdin monoesters (**15**, **16**, **17**) were expected (and found) to be easily saponified to the corresponding verdin diacids, which were reduced by $NaBH_4$ to form rubin diacids (Scheme 2).

As anticipated, saponification of **30**, **32,** and **34** proved difficult or impossible. Using the same conditions as in the conversion of **37** to **36**, refluxing in a 10% solution of NaOH in aqueous ethanol for 4 h, was insufficient for converting **30** to **29**, leaving ∼20% unreacted **30**, and requiring reflux for an additional 8 h. Similarly, **34** was converted to **33**, but **32** resisted saponification. More than a dozen different experiments were attempted to convert rather hydrophobic **32** to **31,** including saponification by aqueous NaOH in refluxing mixtures of ethanol or pyridine, glyme, or diglyme. Heating **32** in DMSO−aqueous NaOH at >100 °C achieved eventual saponification, but the reaction conditions also led to copious quantities of silicate formed by partially dissolving the reaction flask. And since the sodium salt of **31** is insoluble in water, we could not isolate **31** from the silicate. However, by using an S_N2 displacement of the carboxylate anion from the methyl ester by reaction of **32** with anhydrous LiI in refluxing (>170 °C) *s*-collidine,[14] we achieved complete demethylation of the ester and isolated a 99% yield of acid **31** by partially removing the solvent and diluting with aqueous HCl to precipitate the product.

^{13}C NMR Spectra and Molecular Structure. Pairs of mesobilirubin diastereomers involving isomerism based on substitution at the α-position of the C(8) propionic acid and the β'-position of the C(12) propionic acid have been distinguished

(19) MacPhee, J. A.; Dubois, J.-E. *J. Chem. Soc., Perkin Trans. 1* **1977**, 694−696.

(20) Nilson, A.; Carlson, R. *Acta Chem. Scand.* **1980**, *B34*, 621. (b) Bott, K.; Hellmann, H. *Angew. Chem., Int. Ed. Engl.* **1966**, *5*, 870−874. (c) Botteron, D. G.; Shulman, G. P. *J. Org. Chem.* **1962**, *27*, 1059−1061. (d) Traynham, J. G.; Battiste, M. A. *J. Org. Chem.* **1957**, *22*, 1551−1553.

(21) Fuson, R. C.; Walker, J. T. *J. Am. Chem. Soc.* **1930**, *52*, 3269−3275. (b) Newman, M. S.; Connor, H. E. *J. Am. Chem. Soc*. **1950**, *72*, 4002−4003.

(22) McDonald, S. F.; Markovac, A. *Can. J. Chem.* **1965**, *43*, 3247−3252.

(23) Robinson, J. A.; McDonald, E.; Battersby, A. R. *J. Chem. Soc., Perkin Trans. 1* **1985**, 1699−1709.

(24) Fischer, H.; Nenitzescu, C. *Liebigs Ann. Chem.* **1925**, *443*, 113−129.

Table 1. Comparison of ^{13}C NMR Chemical Shifts of Mesobilirubin-XIIIα Analogues **1**−**6** (R—) and **7**−**12** (R···) in 5×10^{-3} M $CDCl_3$ Solutions at 25°C

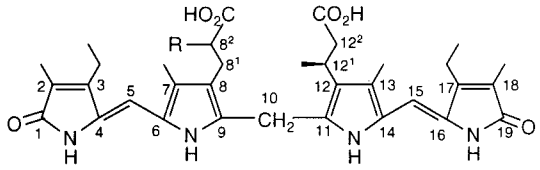

	compound (R)											
carbon	**1** (Me)	**2** (Et)	**3** (*i*-Pr)	**4** (*t*-Bu)	**5** (Ph)	**6** (Bn)	**7** (Me)	**8** (Et)	**9** (*i*-Pr)	**10** (*t*-Bu)	**11** (Ph)	**12** (Bn)
1,19-CONH	174.63	174.61	174.63	174.60	174.72	174.52	174.88	174.90	174.92	174.89	174.87	174.89
	174.94	174.99	175.01	175.18	174.96	174.99	174.91		174.93	175.04	174.99	174.90
2,18	123.62	123.58	123.56	123.58	123.51	123.55	123.41	123.40	123.41	123.38	123.56	123.42
	123.73	123.75	123.76	123.98	123.84	123.68	123.89	123.84	123.82	123.86	123.73	123.80
2,18-CH_3	7.92	7.92	7.91	7.87	7.90	7.93	7.93	7.91	7.90	7.86	7.90	7.93
		7.96	7.96	7.96	7.96	7.96		7.93	7.93	7.92	7.95	
3,17	148.19	148.22	148.23	148.27	148.26	148.22	148.33	148.33	148.35	148.37	148.39	148.32
	148.35	148.40	148.42	148.63	148.48	148.45	148.42	148.45	148.48	148.64	148.54	148.51
3,17-CH_2CH_3	17.81	17.83	17.83	17.84	17.84	17.83	17.83	17.81	17.81	17.80	17.83	17.80
						17.84		17.83	17.84	17.84	17.85	17.85
3,17-CH_2CH_3	14.87	14.87	14.87	14.84	14.85	14.87	14.87	14.88	14.88	14.84	14.85	14.86
		14.89	14.88	14.88	14.90					14.86	14.89	14.87
4,16	128.35	128.36	128.36	128.39	128.44	128.26	128.18	128.16	128.17	128.18	128.38	128.13
	128.38	128.37	128.38	128.44	128.64	128.36	128.29	128.28	128.29	128.36	128.41	128.29
5,15-CH═	100.43	100.47	100.48	100.60	100.37	100.37	100.37	100.38	100.40	100.46	100.42	100.50
	100.57	100.63	100.64	100.71	100.70	100.81	100.51	100.54	100.56	100.69	100.48	100.52
6,14	123.27	123.26	123.24	123.18	123.34	123.26	123.23	123.20	123.20	123.14	123.30	123.21
	123.32	123.32	123.32	123.32	123.47	123.28	123.27	123.25	123.24	123.22	123.45	123.24
7,13	119.31	119.20	119.09	118.86	118.74	119.01	119.17	119.02	118.93	118.67	118.60	118.83
	122.70	122.70	122.71	122.70	122.86	122.73	122.39	122.42	122.44	122.51	122.53	122.48
7,13-CH_3	9.79	9.78	9.77	9.75	9.81	9.73	10.25	10.27	10.29	10.42	10.39	10.06
	10.17	10.21	10.22	10.36	10.31	10.02	11.01	11.01	11.01	11.00	11.03	11.00
8,12	123.93	123.96	123.97	124.08	124.07	123.97	124.18	124.21	124.25	124.30	124.37	124.19
	123.95	124.00	124.04	124.12	124.14	124.00	124.79	124.81	124.83	125.04	124.91	124.76
8^1-CH_2	27.96	25.00	21.23	21.75	28.99	24.53	28.01	25.03	21.23	21.78	29.08	24.53
8^2-CH	39.18	45.52	50.29	54.25	51.07	46.12	39.14	45.46	50.22	54.18	51.02	46.07
8^{21}	19.24	27.02	31.40	33.45	139.77	39.91	19.67	27.07	31.44	33.48	139.79	39.95
8^{22}		11.25	18.97	28.38	127.57	138.68		11.25	18.95	28.37	127.56	138.66
			20.38						20.38			
8^{23}					128.93	129.22					128.95	129.24
8^{24} and 8^{25}					127.47	128.53					127.49	128.53
						126.64						126.66
12^1-CH	28.07	28.08	28.07	28.02	28.06	28.09	26.49	26.49	26.49	26.47	26.51	26.48
12^1-CH_3	19.58	19.37	19.34	19.42	19.22	19.61	21.00	20.99	20.98	20.93	20.98	20.96
12^2-CH_2	38.52	38.65	38.61	38.63	38.47	38.95	39.53	39.53	39.54	39.52	39.54	39.52
8^3,12^3- COOH	178.07	178.05	178.05	177.94	178.10	178.02	179.20	179.18	179.19	179.10	179.22	179.18
	182.35	181.66	181.01	180.41	179.36	180.92	182.29	181.58	180.93	180.29	179.27	180.85
9,11	132.68	132.69	132.73	132.82	132.69	132.64	132.80	132.83	132.85	132.93	132.79	132.86
	133.37	133.41	133.52	133.49	133.57	133.31	133.27	133.35	133.47	133.49	133.46	133.34
10-CH_2	23.94	23.95	23.97	23.94	24.06	23.93	21.98	21.98	22.01	21.96	22.09	21.98

previously by polarity differences. For example, when the substituents are methyl groups, **1** (α*R*,*β*′*S*) is much more polar than **7** (α*S*,*β*′*S*) on silica gel TLC and on reverse phase HPLC.[9d] Even when the α-substituents are electron-withdrawing methoxyl or methylthio groups and the *β*′-substituent is methyl, the (α*R*,*β*′*S*) diastereomer is more polar than the (α*S*,*β*′*S*).[12] In all examples, the configurational assignment was based on knowledge of the absolute configuration of the right half component[9a] and nuclear Overhauser effect (NOE) experiments. As will be shown later, the assignment of configuration of **1**−**12** (Scheme 2) is based initially on the absolute configuration of dipyrrinone precursors (**36** and **37**), and the relative polarity of the diastereomeric rubins was confirmed by $^1H\{^1H\}$-NOE measurements.

The ^{13}C NMR chemical shifts of **1**−**12** (Table 1) were assigned by HMBC experiments and by analogy to previously assigned structures.[9] Aside from the carbon resonances of the various C(8) propionic acid groups, there is considerable similarity in chemical shifts for most of the corresponding carbons of 1−12. Nonetheless, subtle differences can be seen that implicate conformational dissimilarities between pairs of isomers. In particular, (*i*) the C(10)−CH_2 and C(12^1) *β*′-CH resonances are much more deshielded (by ∼1.5 to 2 ppm) and the C(12^2) α′-CH_2 resonances are more shielded (by ∼1 ppm) in **1**−**6** relative to the corresponding diastereomers **7**−**12**, and (*ii*) the methyls at C(7)/C(13) show a greater relative shielding (∼0.5−1 ppm) in **1**−**6** than in the corresponding diastereomers **7**−**12**. In contrast, the carbon resonances in the acid chain at C(8) are scarcely affected, as are the methyls at C(2)/C(18). In **7**−**12**, where the α and *β*′ stereogenic centers have the same chiral sense (for which we use the term: *syn-chiral*),[25] intramolecular nonbonded steric interactions are minimized when the

(25) A reviewer has suggested that a term should be used to indicate the series (**7**−**12**) where the α and *β*′ stereocenters have the same helical sense and a term for when α and *β*′ stereocenters of the series (**1**−**6**) have the opposite helical sense. For the same helical sense, we use the term *syn-chiral*; for the opposite helical sense, we use the term *anti-chiral*. Such terms are a convenient way to allow for the fact that while the *β*′ center has the *S*-configuration in **1**−**12**, *syn-chiral* **7**−**12** do not all have the α-(*S*)-configuration and *anti-chiral* **1**−**6** are not all α(*R*). This "anomaly" is due not to a change in helical sense but to a change in group priority in the CIP rule.

Table 2. Comparison of Selected ^{1}H NMR Chemical Shifts of Mesobilirubin-XIIIα Analogues **1**−**6** (R—) and Their Diastereomers **7**−**12** (R···) in 1×10^{-3} M $CDCl_3$ Solutions at 25 °C

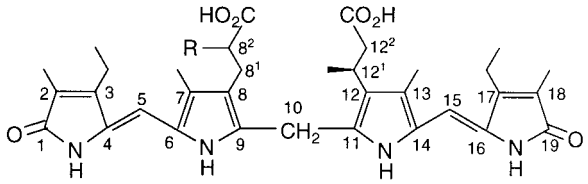

	compound (R)											
proton	**1** (Me)	**2** (Et)	**3** (*i*-Pr)	**4** (*t*-Bu)	**5** (Ph)	**6** (Bn)	**7** (Me)	**8** (Et)	**9** (*i*-Pr)	**10** (*t*-Bu)	**11** (Ph)	**12** (Bn)
8^3,12^3COOH	13.71	13.77	13.46	13.41	13.29	14.04	13.64	13.62	13.61	13.53	13.60	13.62
			13.77	13.67	14.12				13.64	13.60	13.98	13.91
21,24-NHCO	10.45	10.42	10.42	10.31	10.46	10.39	10.49	10.47	10.46	10.34	10.42	10.44
	10.65	10.63	10.62	10.51	10.58	10.60	10.73	10.71	10.70	10.64	10.73	10.69
22,23-NH	8.96	8.94	8.94	8.80	8.97	8.89	9.04	9.02	9.02	8.90	9.05	8.96
	9.29	9.28	9.26	9.19	9.33	9.26	9.08	9.07	9.07	9.00	9.14	9.05
8^1 H_X	2.40	2.44	2.44	2.58	2.65	2.37	2.42	2.47	2.47	2.60	2.66	2.39
	$^3J = 2.4$	$^3J = 2.2$	$^3J = 3.1$	$^3J = 1.7$	$^3J = 2.9$	$^3J = 2.6$	$^3J = 2.5$	$^3J = 3.5$	$^3J = 3.3$	$^3J = 1.7$	$^3J = 3.0$	$^3J = 2.6$
	$^2J = 14.3$	$^2J = 13.7$	$^2J = 14.8$	$^2J = 11.8$	$^2J = 14.7$	$^2J = 14.6$	$^2J = 14.1$	$^2J = 13.5$	$^2J = 14.7$	$^2J = 12.8$	$^2J = 14.8$	$^2J = 14.6$
8^1 H_A	2.88	2.89	2.87	2.88	3.33	2.78	2.90	2.92	2.90	2.89	3.35	2.79
	$^3J = 12.2$	$^3J = 11.6$	$^3J = 12.7$	$^3J = 12.8$	$^3J = 12.7$	$^3J = 11.9$	$^3J = 12.1$	$^3J = 12.2$	$^3J = 12.9$	$^3J = 12.1$	$^3J = 12.7$	$^3J = 12.1$
	$^2J = 14.3$	$^2J = 13.7$	$^2J = 14.8$	$^2J = 11.8$	$^2J = 14.7$	$^2J = 14.6$	$^2J = 14.1$	$^2J = 13.5$	$^2J = 14.7$	$^2J = 12.8$	$^2J = 14.8$	$^2J = 14.6$
8^2 H_B	3.03	2.95	2.93	2.90	4.16	3.22	3.04	2.96	2.93	2.91	4.17	3.24
12^1 $H_{X'}$	3.23	3.24	3.24	3.24	3.26	3.24	3.45	3.45	3.45	3.44	3.47	3.42
12^2 $H_{A'}$	2.70	2.71	2.70	2.70	2.71	2.68	2.70	2.70	2.70	2.69	2.71	2.68
	$^3J = 4.1$	$^3J = 4.4$	$^3J = 4.2$	$^3J = 4.3$	$^3J = 4.2$	$^3J = 4.4$	$^3J = 2.9$	$^3J = 3.0$	$^3J = 2.9$	$^3J = 3.2$	$^3J = 2.9$	$^3J = 3.0$
	$^2J = 18.3$	$^2J = 18.2$	$^2J = 18.3$	$^2J = 18.2$	$^2J = 18.3$	$^2J = 18.3$	$^2J = 18.3$	$^2J = 18.3$	$^2J = 18.3$	$^2J = 18.3$	$^2J = 18.2$	$^2J = 18.3$
12^2 $H_{B'}$	2.99	2.98	2.98	2.97	3.00	2.97	3.09	3.08	3.09	3.07	3.10	3.07
	$^3J = 4.5$	$^3J = 4.6$	$^3J = 4.4$	$^3J = 4.5$	$^3J = 4.4$	$^3J = 4.2$	$^3J = 12.3$	$^3J = 12.3$	$^3J = 12.2$	$^3J = 12.5$	$^3J = 12.4$	$^3J = 12.4$
	$^2J = 18.3$	$^2J = 18.2$	$^2J = 18.3$	$^2J = 18.2$	$^2J = 18.3$	$^2J = 18.3$	$^2J = 18.3$	$^2J = 18.3$	$^2J = 18.3$	$^2J = 18.3$	$^2J = 18.2$	$^2J = 18.3$
10-CH_2	4.20	4.21	4.20	4.14	4.32	4.14	3.99	4.00	4.00	4.00	4.05	3.94
	4.33	4.32	4.32	4.32	4.37	4.26	4.11	4.10	4.09	4.03	4.21	4.02
	$^2J = 15.6$	$^2J = 15.8$	$^2J = 15.6$	$^2J = 15.9$	$^2J = 15.6$	$^2J = 15.7$	$^2J = 15.6$	$^2J = 15.6$	$^2J = 15.6$	$^2J = 15.6$	$^2J = 15.6$	$^2J = 15.6$

pigment adopts the ***M*** (but not the ***P***) helical intramolecularly hydrogen-bonded ridge-tile conformation (Figures 3 and 4).

In the pseudo-*meso* diastereomers **1**−**6**, however, the α and *β*′ stereogenic centers have an opposite chiral sense (for which we use the term: *anti-chiral*)[25] and thus intramolecular steric repulsions are unavoidable in the ridge-tile conformation, either between the *β*′(*S*)-methyl and the C(10)−CH_2 in the ***P***-helical, or between the α-substituent and the C(7) methyl in the ***M***-helical. Hence, the choice of ***M*** or ***P*** chirality is less clear for rubins **1**−**6**. Earlier studies[9d] showed that in **1** the steric requirement of the α(*R*)-CH_3 dominated that of the *β*′(*S*)-CH_3 and thus led to a predominance of the ***P***-helical conformer. This study provided a standard for exploring the relative steric requirements of other groups substituted at the α-carbon, e.g., OCH_3 and SCH_3, which have smaller *A*-values than CH_3.[2] In our intramolecularly hydrogen bonded rubin template, we found that while α-OCH_3 did indeed have a much smaller steric requirement than α-CH_3, interestingly, that of α-SCH_3 was larger.[12] The steric demand of SCH_3 is apparently larger than that of CH_3, counter to what the *A*-values imply, probably because the longer C−S (vs C−C) bond leads to a more severe buttressing of the α-SCH_3 group as compared to the α-CH_3.

Conformation from ^{1}H NMR. For purposes of eliciting information on the conformation of bilirubins, the ^{1}H NMR chemical shifts of the dipyrrinone NHs and the vicinal coupling constants in the propionic acid chains are of special interest. When coupled with NOE experiments, these data are a particularly good diagnostic for detecting intramolecular hydrogen bonding and confirming the presence of ridge-tile conformations.[9,10,26,27] The data of Table 2 indicate pyrrole NH resonances near 9 ppm, an upfield shift characteristic of hydrogen bonding in a ridge-tile conformation where each pyrrole NH lies above the neighboring pyrrole ring and is diamagnetically shielded by it.[9,10,12,26,27] In contrast, when the two dipyrrinones form a planar intermolecularly hydrogen-bonded association complex, the pyrrole NH resonates at ∼10 ppm.[9,26,27] The deshielded lactam NH resonances near 10−11 ppm are also in agreement with intramolecular hydrogen-bonding, as shown previously for **1** and **7**[9d] and other well characterized bilirubins.[9,27]

Vicinal coupling constants in the propionic acid chains of **1**−**12**, such as those of **5** and **11** in Figure 5, provide further insight into the importance of intramolecular hydrogen bonding to pigment conformation. As found previously in the ^{1}H NMR spectra of **1** and **7**[9d,12] in $CDCl_3$, the $-C_\beta H_2-C_\alpha HR$- and $-C_{\beta'}H$-(Me)-$C_{\alpha'}H_2-$ segments of the propionic acid chains of **2**−**6** and **8**−**12** exhibit well-defined ABX spin systems with coupling constants characteristic of a fixed staggered geometry, as shown in Figure 6. In $(CD_3)_2SO$, these segments exhibit averaged coupling constants characteristic of greater conformational flexibility/motion in the propionic acid groups. Significantly, the $^3J_{AB}$ (12.1−12.9 Hz) and $^3J_{B'X'}$ (12.2−12.5 Hz) coupling constants of **7**−**12** are large; whereas, those of $^3J_{BX}$ (1.7−3.5 Hz) and $^3J_{A'X'}$ (2.9−3.2 Hz) are small, indicating an *anti*-periplanar orientation of the H_A and H_B (or $H_{B'}$ and $H_{X'}$) and the *syn*-clinal orientation of H_B and H_X (or $H_{A'}$ and $H_{X'}$), as shown in Figure 6B. This is consistent with the α and *β*′ substituents of the propionic acids working in concert sterically to dictate an ***M***-helical ridge-tile conformation (Figures 3 and 4). However, in **1**−**6** the α-substituent and the *β*′(*S*) methyl group work in opposition, each attempting to dictate, teeter-totter fashion, the ***M*** or ***P*** helical conformation. In each case

(26) Dörner, T.; Knipp, B.; Lightner, D. A. *Tetrahedron* **1997**, *53*, 2697−2716.

(27) Kar, A.; Lightner, D. A. *Tetrahedron*, **1998**, *54*, 12671−12690.

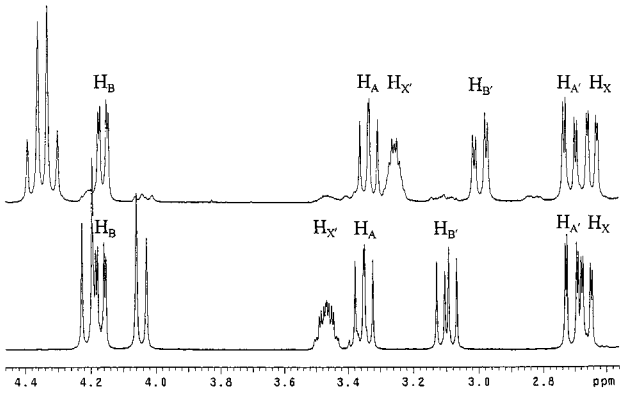

Figure 5. Partial 500 MHz ^{1}H NMR spectra showing the nicely resolved ABX and A′B′X′ spin systems of the C(8)−$C_\beta H_A H_X$−$C_\alpha H_B$R−CO_2H and C(12)−$C_{\beta'} H_{X'}$(CH_3)−$C_\alpha H_{A'} H_{B'}$−CO_2H propionic acids of **5** (upper spectrum) and **11** (lower spectrum) in $CDCl_3$ at 25 °C. (R = Ph in **5** and **11**.)

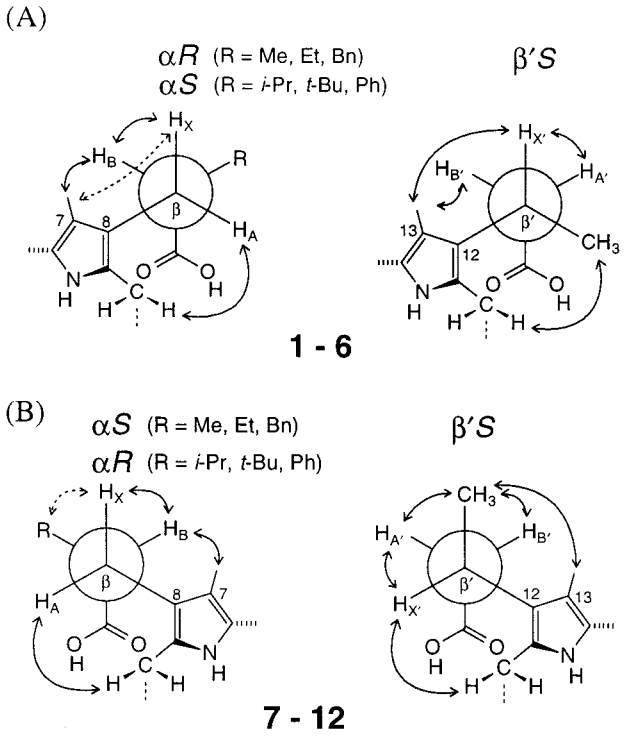

Figure 6. Nuclear Overhauser effects (NOEs) found in the rubin (A) *anti-chiral* ***P***-helical or (B) *syn-chiral* ***M***-helical conformations that lock the −$C_\beta H_2$−C_αHR− and −$C_{\beta'}$HMe−$C_{\alpha'} H_2$− segments of the propionic acid groups of **1**−**12** in the conformations shown. The ABX spin systems are labeled accordingly, and the ^{1}H{^{1}H}-NOEs observed are indicated by double-headed curved arrows. Coupling constants characteristic of restricted rotation found in the fixed staggered propionic acid geometry are shown in Table 2 and are characteristic of intramolecularly hydrogen-bonded ridge-tile conformations (Figures 3 and 4).

the steric demand of the α-group is seen to overcome that of the *β*′(*S*)-methyl. Thus, the $^3J_{AB}$ couplings are again large (11.6−12.8 Hz) but neither $^3J_{A'X'}$ nor $^3J_{B'X'}$ is large (4.1−4.6 Hz). The coupling constants indicate that the C(8) propionic chain maintains the mirror image fixed staggered geometry found in **7**−**12** while the C(12) propionic acid chain of **1**−**6** adopts a fixed staggered conformation in which $H_{B'}$ and $H_{X'}$, as well as $H_{A'}$ and $H_{X'}$ are now *syn*-clinal (Figure 6A, cf. $H_{B'}$ signals in Figure 5). These data indicate a preference for the ***P***-helicity conformation in **1**−**6** and a greater steric demand exerted by the α groups (Me, Et, *i*-Pr, *t*-Bu, Ph, Bn) than a *β*′-Me. As we shall see, this fact offers a way to compare the relative steric demand of the α-substituents.

Nuclear Overhauser Effects and 3D Structure. Application of the pulsed field gradient method for measuring transient ^{1}H-{^{1}H} nuclear Overhauser effects (NOEs)[28] showed a very strong NOE between the dipyrrinone lactam and pyrrole NHs, confirming the *syn-Z* stereochemistry about the C(4)═C(5) and C(15)═C(16) bonds and also matching and identifying each pair of dipyrrinone lactam and pyrrole NH signals in **1**−**12**. From these assignments and from HMBC and HMQC measurements, we were thus able to assign all of the proton and carbon signals. Using steady-state NOE difference spectroscopy and irradiating the lactam N(21)−H protons, we were able to detect 2−4% signal enhancements of the C(12) propionic acid COOH signals in **1**−**12**, and by irradiating the lactam N(24)−H protons, we detected enhancements of the C(8) propionic acid COOH signals. These data indicate the close proximity of the COOH and relevant lactam NH groups, as one would find in the ridge-tile conformation (Figures 3 and 4).

Strong supporting evidence for the ***P***-helical intramolecularly hydrogen-bonded ridge-tile conformation in **1**−**6**, and the ***M***-helical in **7**−**12**, comes from NOE measurements in $CDCl_3$ involving the propionic acid hydrogens. In **1**−**6** one find an NOE (i) between the α-H_B of the C(8) propionic chain and the C(7)−CH_3 and (ii) between the *β*-H_A and only one of the C(10)−CH_2s. In **7**−**12**, corresponding NOEs are found in the C(8) propionic acid chain between α-H_B and the C(7)−CH_3 and between *β*-H_A and one of the C(10)−CH_2s. These data indicate a close proximity of the cited protons in **1**−**12** (Figures 4 and 6). NOEs in the C(12) propionic acid chain of **1**−**6** are seen between the *β*′-$H_{X'}$ and the C(13)−CH_3 and between the *β*′-CH_3 and the other C(10)−CH_2 proton, consistent with the conformation shown in Figure 6A, where the *β*′-CH_3 is sterically compressed into the C(10)−CH_2 group. In clear contrast, in **7**−**12** NOEs are seen between the *β*′-CH_3 and the C(13)−CH_3 and between *β*′-$H_{X'}$ and one of the C(10)−CH_2s, consistent with the conformation shown in Figure 6B, where the *β*′-CH_3 does not exsert into the C(10)−CH_2 group. Taken collectively, these data support the stereochemical relationships shown in Figure 6 for the ***P***-helicity conformation in **1**−**6**, and they are incompatible with the ***M***-helicity. For the latter, one would expect NOEs (i) between the α-R group and the C(7)−CH_3 and (ii) between the *β*′-$H_{X'}$ and a C(10)−CH_2 hydrogen, but these are not observed.

Stereochemistry from Circular Dichroism Spectroscopy. The effectiveness of the *syn-chiral* [α(*S*)-Me, -Et, and -Bn and α(*R*)-*i*-Pr, -*t*-Bu, and -Ph] groups in reinforcing the conformational bias of the *β*′(*S*)-Me toward displacing the conformational equilibrium of Figures 3 and 4 in favor of the ***M***-helical conformation in rubins **7**−**12**, or of the *anti-chiral* groups in counteracting it and causing **1**−**6** to adopt a ***P***-helical conformation, may be detected and analyzed by CD spectroscopy. Intense bisignate Cotton effects are seen for the long wavelength transition(s) of **1**−**12** (Figures 7 and 8). The bisignate Cotton effects have their origins not simply from the presence of the α and *β*′ stereogenic centers on the propionic acids, or the electronic perturbation of the nearby dipyrrinone chromophores, but from the influence of these centers on the pigment conformational stereochemistry. Although one would expect only a weak, monosignate CD associated with a $\pi \rightarrow \pi^*$ excitation from a dipyrrinone chromophore perturbed by dissymmetric vicinal action, when two dipyrrinone chromophores

(28) Stott, K.; Keeler, J.; Van, Q. N.; Shaka, A. J. *J. Magn. Reson.* **1997**, *125*, 302−324.

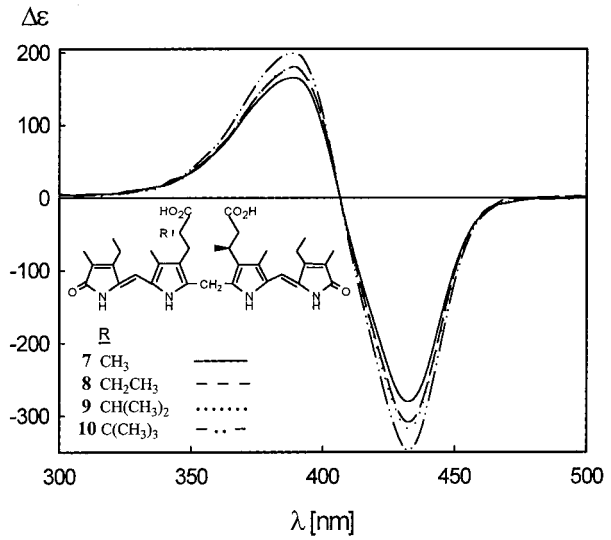

Figure 7. Circular dichroism spectra of ~1.5 × 10^{-5} M mesobilirubin analogues **7**−**10** in CH_2Cl_2 solvent at 22 °C.

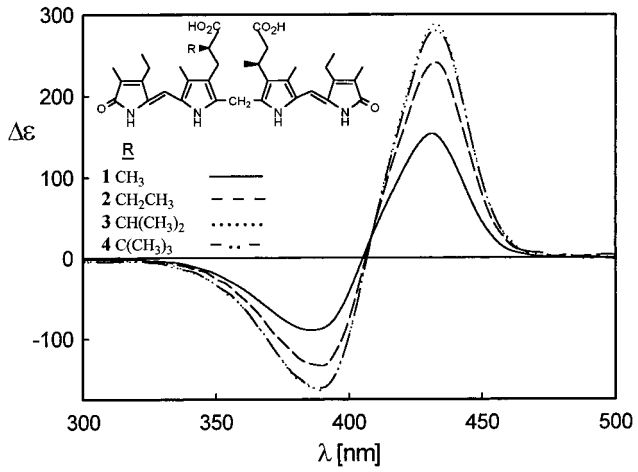

Figure 8. Circular dichroism spectra of ~1.5 × 10^{-5} M mesobilirubin analogues **1**−**4** in CH_2Cl_2 solvent at 22 °C.

interact by coupling locally excited $\pi \rightarrow \pi^*$ transitions (electric transition dipole coupling),[6,8c,9] one would expect to observe bisignate spectra characteristic of an exciton system.[11] The component dipyrrinone chromophores of the bichromophoric rubins have strongly allowed long-wavelength electronic transitions ($\epsilon_{410}^{max} \sim 37\,000$) but only a small interchromophoric orbital overlap in the ridge-tile conformation (Figure 3). They are nicely oriented to interact by electrostatic interaction of the local transition moment dipoles, which are polarized along the long axis of each dipyrrinone, i.e., resonance splitting. Such intramolecular exciton interaction produces two long-wavelength transitions in the UV−vis spectrum and two corresponding bands in the CD spectrum. One band is higher in energy, and one is lower in energy, with the splitting being dependent on the strength and relative orientation of the dipyrrinone electric dipole transition moments (Figure 3). When observed by UV−vis spectroscopy, the two electronic transitions overlap to give the typically broadened and sometimes split long-wavelength absorption band found in bilirubins. In the CD spectra, however, the two exciton transitions are oppositely signed, and thus, bisignate spectra are typically seen−as predicted by theory.[6,8c,11]

From exciton chirality theory,[11] the signed order of the bisignate CD Cotton effects may be used to predict the relative orientation of the two electric dipole transition moments, one from each dipyrrinone of the rubin. Thus, a negative exciton chirality (long-wavelength negative Cotton effect followed by a positive short-wavelength Cotton effect) corresponds to a negative torsion angle between the transition dipoles. On the other hand, a positive exciton chirality (long-wavelength positive Cotton effect followed by a negative short-wavelength Cotton effect) corresponds to a positive torsion angle. Accordingly, the ***M***-helicity conformer of Figure 3 is predicted to have a negative exciton chirality, and the ***P***-helicity is predicted to have a positive exciton chirality.

In nonpolar solvents, such as hexane, CCl_4, CH_2Cl_2, and $CHCl_3$, that preserve intramolecular hydrogen bonding and hence the ridge-tile stereochemistry, the steric compression model (Figure 4), predicts that the *syn-chiral* stereochemistry of pigments **7**−**12** will work in concert to drive the ***M*⇆*P*** equilibrium toward ***M***. And the predominance of the ***M***-helical conformer is confirmed by the intense negative exciton chirality CD curves (Figure 7 and Table 3) of **7**−**12**. However, when the stereochemistry at the α-carbon is inverted, as in **1**−**6**, the α-group is expected to resist the efforts of the *β′*(*S*)-methyl to dictate an ***M***-helicity conformer, thus creating a molecular teeter-totter. In **1**−**6**, with *anti-chiral* stereochemistry, it is clear from their positive exciton chirality CD spectra (Figure 8 and Table 3) in nonpolar solvents, where the ridge-tile conformation is preserved, that substituents at the α-carbon dominate the *β′*-(*S*)-CH_3 group. Given the earlier observation that an α(*R*)-CH_3 dominates a *β′*(*S*)-CH_3,[9d] the fact that even larger α-substituents counteract and dominate the influence of a *β′*(*S*)-CH_3 is qualitatively in keeping with their relative steric sizes, based on their *A*-values: *t*-Bu > Ph > *i*-Pr > Et > Bn > Me.[2,3,29]

Although the Cotton effect intensities of **1**−**12** are large in nonpolar solvents (Table 3), they are generally reduced in polar solvents, especially those capable of interfering with the intramolecular hydrogen bonding motif of Figures 3 and 4. In CH_3OH, for example, the CD intensities of **7**−**12** where the α and *β′* stereochemistry acts in concert (*syn-chiral*) remain moderately strong. However, where the stereochemistry at α and that at *β′* act in opposition (*anti-chiral*), the CD intensities of **1**−**6** are rather weak. In contrast, in the polar aprotic and non-hydrogen bonding solvents such as CH_3CN, the CD intensities of **1**−**12** are considerably larger than in CH_3OH, especially among **1**−**6**, but the CD intensities are still well below those in nonpolar solvents. Where some intramolecular hydrogen bonding is maintained, as in CH_3CN, the CD values can be moderately large even when the α and *β′* groups are *anti-chiral*. However, when the polar aprotic solvent is capable of participating in hydrogen bonding as in $(CH_3)_2SO$, the Cotton effect intensities of **1**−**12** drop to <10% of the values in nonpolar solvents, and in **1**−**10** the signs are reversed. Solvent molecules are apparently involved in the network of intramolecular hydrogen bonds, and NMR[30] and CD[31] studies suggest that the propionic acids are linked to the dipyrrinones by $(CH_3)_2SO$. It seems probable that the favored folded conformation has become somewhat more open (larger *θ* angle in Figure 3) to accommodate attachment of the solvent molecules. Such a conformational change lessens the intramolecular steric buttressing that so effectively directs the ***M*⇆*P*** equilibrium toward either **M** or **P**. With the smaller equilibrium constant, Δϵ values drop substantially. When firm hydrogen bonding is not maintained or is expanded by intercalation of solvent molecules, the allosteric model that allows one to make quantitative evaluations

(29) Juaristi, E.; Labastida, V.; Antúnez, S. *J. Org. Chem.* 2000, *65*, 969−973; **1991**, *56*, 4802−4804.
(30) Kaplan, D.; Navon, G. *Isr. J. Chem.* **1983**, *23*, 177−186.
(31) Trull, F. R.; Shrout, D. P.; Lightner, D. A. *Tetrahedron* **1992**, *48*, 8189−8198.

Table 3. Solvent Dependence of the Circular Dichroism and Ultraviolet−Visible Spectral Data from ~1.5 × 10^{-5} M Solutions of Mesobilirubin-XIIIα Analogues **1**−**12** at 22 °C

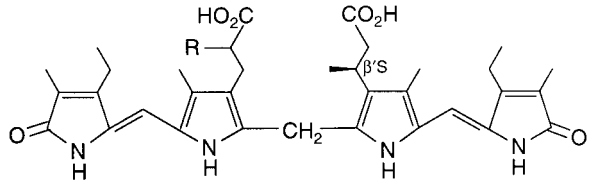

pigment				CD			UV	
no.	R[a]	solvent (ϵ[b])	**A**[c]	$\Delta\epsilon_1^{max}$ (λ_1)	λ at $\Delta\epsilon = 0$	$\Delta\epsilon_2^{max}$ (λ_2)	ϵ^{max}	λ (nm)
1	Me	hexane	+277	+179 (427)	400	−98 (384)	59 300	428
2	Et	(1.9)	+427	+294 (429)	402	−132 (385)	60 900	435
3	*i*-Pr		+506	+344 (430)	403	−162 (389)	56 300	435
4	*t*-Bu		+513	+348 (430)	403	−165 (388)	59 800	432
5	Ph		+418	+284 (428)	401	−134 (386)	59 000	435
6	Bn		+378	+260 (430)	403	−118 (388)	57 700	435
7	*Me*		*−512*	*−346 (430)*	*403*	*+166 (389)*	*63 800*	*432*
8	*Et*		*−588*	*−403 (430)*	*408*	*+185 (389)*	*63 000*	*433*
9	*i*-Pr		*−585*	*−401 (430)*	*403*	*+184 (389)*	*64 100*	*436*
10	*t-Bu*		*−640*	*−439 (430)*	*403*	*+201 (389)*	*62 300*	*433*
11	*Ph*		*−617*	*−425 (429)*	*402*	*+192 (389)*	*64 300*	*432*
12	*Bn*		*−530*	*−363 (431)*	*403*	*+167 (390)*	*57 600*	*435*
1	Me	CCl_4	+272	+181 (433)	405	−91 (390)	58 300	434
2	Et	(2.2)	+411	+282 (434)	407	−129 (392)	59 700	438
3	*i*-Pr		+488	+334 (434)	407	−154 (393)	55 700	440
4	*t*-Bu		+497	+336 (434)	407	−161 (392)	59 200	437
5	Ph		+433	+295 (433)	406	−138 (390)	60 600	436
6	Bn		+370	+257 (434)	407	−113 (393)	58 700	433
7	*Me*		*−490*	*−331 (434)*	*407*	*+159 (393)*	*62 400*	*436*
8	*Et*		*−543*	*−371 (434)*	*407*	*+172 (393)*	*60 900*	*437*
9	*i-Pr*		*−548*	*−375 (434)*	*407*	*+173 (392)*	*61 700*	*438*
10	*t-Bu*		*−614*	*−416 (434)*	*407*	*+198 (392)*	*61 500*	*437*
11	*Ph*		*−579*	*−396 (433)*	*406*	*+183 (393)*	*62 800*	*436*
12	*Bn*		*−506*	*−346 (435)*	*408*	*+160 (393)*	*56 800*	*438*
1	Me	$CHCl_3$	+250	+151 (428)	402	−99 (384)	56 900	424
2	Et	(4.7)	+367	+235 (433)	407	−132 (390)	56 700	434
3	*i*-Pr		+436	+280 (434)	408	−156 (390)	52 300	432
4	*t*-Bu		+450	+285 (434)	408	−165 (390)	58 000	432
5	Ph		+347	+223 (432)	406	−124 (387)	58 200	431
6	Bn		+318	+205 (433)	407	−113 (389)	54 800	434
7	*Me*		*−455*	*−288 (434)*	*407*	*+167 (389)*	*58 200*	*432*
8	*Et*		*−502*	*−322 (435)*	*408*	*+180 (390)*	*58 400*	*434*
9	*i-Pr*		*−503*	*−322 (435)*	*408*	*+181 (390)*	*57 900*	*433*
10	*t-Bu*		*−550*	*−351 (434)*	*407*	*+199 (390)*	*57 900*	*434*
11	*Ph*		*−513*	*−331 (434)*	*407*	*+182 (390)*	*58 600*	*432*
12	*Bn*		*−462*	*−298 (435)*	*408*	*+164 (391)*	*53 500*	*432*
1	Me	CH_2Cl_2	+243	+154 (432)	405	−89 (386)	58 000	430
2	Et	(8.9)	+374	+241 (433)	406	−133 (389)	57 300	431
3	*i*-Pr		+453	+289 (433)	407	−164 (389)	52 700	432
4	*t*-Bu		+441	+280 (432)	407	−161 (388)	57 700	430
5	Ph		+362	+231 (431)	405	−131 (388)	58 700	431
6	Bn		+351	+228 (432)	406	−123 (388)	57 100	431
7	*Me*		*−445*	*−280 (432)*	*407*	*+165 (389)*	*58 700*	*430*
8	*Et*		*−489*	*−308 (433)*	*407*	*+181 (389)*	*57 400*	*432*
9	*i-Pr*		*−498*	*−318 (433)*	*407*	*+180 (389)*	*58 400*	*433*
10	*t-Bu*		*−546*	*−347 (433)*	*407*	*+199 (389)*	*58 200*	*431*
11	*Ph*		*−526*	*−331 (432)*	*406*	*+195 (388)*	*58 900*	*431*
12	*Bn*		*−447*	*−284 (433)*	*407*	*+163 (389)*	*53 000*	*432*
1	Me	CH_3OH	+39	+24 (424)	397	−15 (376)	57 700	422
2	Et	(32.6)	+26	+15 (422)	394	−11 (383)	56 600	424
3	*i*-Pr		+10	+6 (424)	396	−4 (389)	63 500	421
4	*t*-Bu		−16	−11 (417)	392	+5 (373)	58 000	422
5	Ph		+184	+110 (425)	399	−74 (382)	58 400	424
6	Bn		+89	+55 (425)	397	−34 (382)	57 200	422
7	*Me*		*−370*	*−223 (430)*	*404*	*+147 (385)*	*58 900*	*425*
8	*Et*		*−414*	*−251 (429)*	*404*	*+163 (385)*	*58 600*	*423*
9	*i-Pr*		*−387*	*−237 (430)*	*404*	*+150 (386)*	*56 900*	*425*
10	*t-Bu*		*−416*	*−252 (429)*	*404*	*+164 (385)*	*59 400*	*424*
11	*Ph*		*−451*	*−273 (429)*	*403*	*+178 (386)*	*60 200*	*424*
12	*Bn*		*−386*	*−234 (429)*	*404*	*+152 (386)*	*53 700*	*425*

Table 3. (Continued)

pigment				CD			UV	
no.	R[a]	solvent (ϵ^b)	**A**[c]	$\Delta\epsilon_1^{max}$ (λ_1)	λ at $\Delta\epsilon = 0$	$\Delta\epsilon_2^{max}$ (λ_2)	ϵ^{max}	λ (nm)
1	Me	CH_3CN	+146	+91 (428)	403	−55 (385)	55 200	420
2	Et	(36.2)	+204	+130 (430)	404	−74 (387)	52 800	415
3	*i*-Pr		+306	+195 (429)	404	−111 (387)	60 200	420
4	*t*-Bu		+238	+149 (430)	405	−89 (386)	52 200	415
5	Ph		+236	+149 (427)	402	−87 (381)	53 600	422
6	Bn		+186	+120 (429)	405	−66 (386)	53 400	420
7	*Me*		*−413*	*−258 (429)*	*403*	*+155 (384)*	*57 300*	*424*
8	*Et*		*−469*	*−298 (428)*	*403*	*+171 (385)*	*56 300*	*425*
9	*i-Pr*		*−457*	*−289 (428)*	*403*	*+168 (385)*	*54 500*	*425*
10	*t-Bu*		*−512*	*−325 (428)*	*403*	*+187 (384)*	*56 200*	*423*
11	*Ph*		*−478*	*−302 (428)*	*403*	*+176 (384)*	*57 800*	*424*
12	*Bn*		*−434*	*−275 (429)*	*403*	*+159 (385)*	*52 000*	*425*
1	Me	$(CH_3)_2SO$	−56	−25 (425)	401	+31 (382)	62 500	428
2	Et	(46.5)	−46	−26 (424)	397	+20 (380)	61 700	430
3	*i*-Pr		−69	−32 (428)	400	+37 (385)	66 900	429
4	*i*-Bu		−23	−9 (420)	403	+14 (381)	56 200	426
5	Ph		−21	−4 (433)	412	+17 (385)	60 400	427
6	Bn		−36	−24 (420)	392	+12 (375)	60 500	429
7	*Me*		*+26*	*+15 (425)*	*395*	*−11 (379)*	*60 000*	*428*
8	*Et*		*+29*	*+15 (420)*		*+14 (402)*	*60 700*	*429*
9	*i-Pr*		*+44*	*+28 (424)*	*396*	*−16 (377)*	*58 200*	*429*
10	*t-Bu*		*+34*	*+21 (428)*	*394*	*−13 (383)*	*56 800*	*426*
11	*Ph*		*−50*	*−27 (426)*	*403*	*+23 (382)*	*60 800*	*427*
12	*Bn*		*−18*	*−2 (445)*	*438*	*+16 (390)*	*57 100*	*429*

[a] **1**−**6** have the same sense of absolute configuration at the α-carbon, nominally *R*, which is opposite to *β′S*-CH_3; **7**−**12** have the same sense of absolute configuration at the α-carbon (nominally *S* and opposite to that of **1**−**6**) and the *β′*-carbon. R groups of the latter are in italics. [b] Dielectric constant from: Gordon, A. J.; Ford, R. A. *The Chemist's Companion*; Wiley: New York, 1972; pp 4−8. [c] Exciton coupling CD amplitude, $\mathbf{A} = \Delta\epsilon_1^{max}(\lambda_1) - \Delta\epsilon_2^{max}(\lambda_2)$.

of steric buttressing is compromised, and thus, we focus our analysis of such on CD data from the nonpolar solvents of this study.

Conformational Analysis and Steric Size. As found by ^{1}H NMR and CD, **1**−**12** are intramolecularly hydrogen bonded and adopt an ***M***- or ***P***-helicity conformation in nonpolar solvents. In **7**−**12** (Scheme 2), the α- and *β′*(*S*)-stereocenters have the same chiral sense (*syn-chiral*) and thus the α-subtituent and *β′*-(*S*)-methyl act cooperatively to reinforce each other in displacing the ***M*⇆*P*** equilibrium of Figure 4 toward ***M***. In **1**−**6**, however, the α- and *β′*(*S*)-stereocenters have the opposite chiral sense (*anti-chiral*). Thus the α-substituent and *β′*(S)-methyl act in opposition, each "weighing in" on the ***M*⇆*P*** equilibrium, "teeter-totter" fashion, with the α-substituent proving dominant over a *β′*-CH_3, hence a predominance of the ***P***-helical conformation. It is this molecular teeter-totter that serves as the equivalent of the axial chair⇆equatorial chair equilibrium of substituted cyclohexanes. Both are templates from which information on group steric size may be extracted.

To evaluate the relative steric size of an α-substituent from the bilirubin molecular teeter-totter, we use the CD exciton couplet intensity amplitude:[11] $\mathbf{A} = \Delta\epsilon_1^{max}(\lambda_1) - \Delta\epsilon_2^{max}(\lambda_2)$. Although the Cotton effect intensity of a single electronic transition may be expressed quantitatively by its integrated area (rotatory strength), similarities between CD curve shapes (Figures 7 and 8) arising from two interacting excited states generally allow one simply to use the sum of the absolute values of $\Delta\epsilon^{max}$ at the two λ^{max} when analyzing exciton CD spectra quantitatively.[11] This is, however, only approximation. Thus, in comparing the CD amplitudes of **7**−**12** in the four nonpolar solvents *n*-hexane, CCl_4, $CHCl_3$, and CH_2Cl_2 (Table 3), solvents that do not interfere significantly with hydrogen bonding, we find negative amplitudes (**A**) that fall within a narrow range; e.g., **A** varries from −455 and −550 in $CHCl_3$. Compounds in decreasing order of **A**: **10** (−550) > **11** (−513) ∼ **9** (−503) ∼ **8** (−502) > **12** (−462) ∼ **7** (−455). These data suggest a ranking of steric size *t*-Bu > Ph ∼ *i*-Pr ∼ Et > Bn ∼ Me that is similar to but not exactly the order of steric size from conformational *A*-values: *tert*-butyl > phenyl > isopropyl > ethyl ∼ benzyl ∼ methyl.[2,3,29]

The difference between the largest CD amplitude of **7**−**12** is only ∼90 $\Delta\epsilon$ units, in $CHCl_3$ and CH_2Cl_2, and it is not much larger in CCl_4 and *n*-hexane (Table 3). It is not quite clear that there should be any difference in **A**, especially since **7**−**12** each reside firmly in the ***M***-helicity conformation by virtue of the α-substituent group and *β′*(*S*)-methyl working concerted by, as dictated by the *syn-chiral* stereochemistry. The differences might reflect either small distortions in the ridge-tile template or an incomplete displacement from ***P*** to ***M*** helical conformations.

In contrast, a more than doubling of the CD amplitude difference is observed in pigments **1**−**6** in the nonpolar solvents. Here the steric demand of the α-substituent is pitted against that of the *β′*(*S*)-methyl, with the former dictating a ***P***-helical conformation and the latter an ***M***. In all cases the α-substituent dominates the *β′*-methyl, thus giving the inverted, positive exciton chirality CD spectra seen in Figure 8. In the dominant ***P***-helical conformation the *β′*(*S*)-methyl is buttressed by the C(10)−CH_2, but if the ***M***-helical conformation had been dominant, the α-substituent would exsert into the C(7)−CH_3. The latter situation apparently creates much more severe steric compression than the former−even when the α-substituent is as small as methyl. As might be expected in the molecular teeter-totter, the most intense exciton CD couplets of the ***P***-helical rubins of **1**−**6** in nonpolar solvents are found with the bulkiest R groups. The CD **A**-values of Table 3 in a quantitative assessment of α-R group steric size in $CHCl_3$ are as follows: **4** (450) ∼ **3** (436) > **2** (367) > **5** (347) > **6** (318) > **1** (250). In the other nonpolar solvents, **3** and **4** consistently exhibited the largest CD **A**-values (Table 4), which were generally within 5% of each other. This surprising observation would seem to indicate that isopropyl and *tert*-butyl have the same steric size, which is counterintuitive. The CD **A**-values for **5** in our nonpolar

Table 4. Comparison of Exciton Chirality **A**-Values and Conformational *A*-Values as Indicators of Functional Group Steric Size in Compounds **1**−**6**

	exciton chirality CD **A**-values[a]				conformational *A*-values[b]	rel steric size from	
	n-hexane	CCl_4	$CHCl_3$	CH_2Cl_2		*A*-values	**A**-values[c]
$C(CH_3)_3$	+513	+497	+450	+441	4.9	2.80	1.81−1.85
C_6H_5	+418	+433	+347	+362	2.87	1.65	1.39−1.59
$CH(CH_3)_2$	+506	+488	+436	+453	2.21	1.27	1.74−1.86
CH_2CH_3	+427	+411	+367	+374	1.79	1.03	1.47−1.54
$CH_2C_6H_5$	+378	+370	+318	+351	1.76	1.01	1.27−1.44
CH_3	+277	+272	+250	+243	1.74	1.00	1.00

[a] From Table 3. [b] From ref 2 (Table 2.2) and ref 29 by NMR: CH_3, CH_2CH_3, $CH(CH_3)_2$ ($CFCl_3$–$CDCl_3$, 300 K), $CH_2C_6H_5$ (CD_2Cl_2, 202 K), $C(CH_3)_3$ (CD_2Cl_2, 153 K), C_6H_5 (CD_2Cl_2, 173 K). [c] Based on CD **A**-values, uncorrected for minor percents of ***M***-helical isomer in **1** (22%), **2** (9%), **5** (8%), and **6** (6%), as detected by ^{1}H NMR in $CDCl_3$. In this solvent, no ***M***-helical isomers could be detected in **3** and **4**.

solvents are consistently less than those of **3** and **4**, generally about the same as **2**, but more than those of **1** and **6**. The CD **A**-values of **1**−**6** thus indicate that phenyl and ethyl are about the same size, that ethyl is larger than benzyl, and both are significiantly larger than methyl. Conformational *A*-values indicate that ethyl, benzyl, and methyl are comparable in steric size. Thus, as determined by the more competitive *anti-chiral* systems **1**−**6**, their CD **A**-values suggest an apparent order for steric size: *tert*-butyl ∼ isopropyl > ethyl ∼ phenyl > benzyl > methyl.

While this ranking does not quite correspond to the relative steric size from conformational *A*-values, *tert*-butyl > phenyl > isopropyl > ethyl ∼ benzyl ∼ methyl,[29] the differences lie most significantly with the isopropyl, phenyl, and ethyl groups. Whether such differences can be attributed to entropy factors or to deformation of the molecular framework is at present unclear. Template mutability is always a concern. For example, the chair cyclohexane template (Figure 1) is not rigid but deformable within certain limits,[3] and any ring deformation caused by one axial group (e.g., *tert*-butyl) would not necessarily be the same as that caused by another (e.g., isopropyl). Recognition of the intrinsic quantitative aspects of steric size might also be compromised in the sterically congested bilirubin template of **1**−**6**, where potential deformation of the ridge-tile template (Figure 4) caused by a *tert*-butyl group might not be matched by an isopropyl, thus lead to a mismatch in the relative order of the group steric size.

Concluding Comments

The relative steric size of common functional groups, *tert*-butyl ∼ isopropyl > ethyl ∼ phenyl > benzyl > methyl, follows from exciton chiraltiy CD **A**-values using a novel conformational model based on the interconverting conformational enantiomers of bilirubin (Figure 3). In the bilirubin template, steric size is determined by head-to-head steric compression. The order differs somewhat from that (*tert*-butyl > phenyl > isopropyl > ethyl ∼ benzyl ∼ methyl) obtained from conformational *A*-values and the chair cyclohexane template, where steric interaction is dominated by gauche interactions.

Acknowledgment. We thank the National Institutes of Health (Grant HD-17779) for support of this work. S.E.B. is on leave from the Institute of Organic Chemistry, Bulgarian Academy of Sciences, Sofia, Bulgaria.

Supporting Information Available: Text providing the Experimental Section, including syntheses of all new compounds. This material is available free of charge via the Internet at http://pubs.acs.org.

JA002069C